

Supporting Information

All-optical tunable plasmonic nano-aggregations for surface-enhanced raman scattering

Lei Chen,^a Wei Liu,^a Dongyi Shen,^a Yuehan Liu,^b Zhihao Zhou,^b Xiaogan Liang,^c and Wenjie Wan^{*ab}

SI-1. Experimental section

Sample Preparation: The gold nanospheres used in the experiments are purchased from Cytodiagnosics. The colloidal gold particles suspended in water is slightly diluted with deionized water to reach a concentration of 10^{-9} M. Crystal violet (CV) is chosen as the probe molecule because it has a low fluorescence quantum yield.¹ CV powder is dissolved in distilled water to prepare stock solution of 0.1 M Stock solutions. Samples in a wide range of CV concentrations ($10^{-1} \sim 10^{-7}$ M) are prepared. An aliquot of gold colloid solution is sonicated for 15 min in order to reduce unnecessary aggregation, before adding the dye to the required final concentration. The mixed samples are sonicated for another 15 min in order to avoid adsorbing. Experiments are conducted on samples covered with deionized water. A drop of colloidal solution ($\sim 100 \mu\text{L}$) is injected into the sample cell consist of two cleaned coverslips.

Surface-enhanced Raman Scattering Microscop: A home-built Raman spectrometer constructed around an inverted microscope is used for these studies. Samples are illuminated by a 532 nm and 1064 nm laser beam which are focused at the detection plane of an objective (100 \times , NA. 1.25). Polarization of the green laser is controlled by a half-wave and a quarter-wave plate. Slightly collimated white light from a halogen lamp is illuminated onto a sample from the opposite of the objective. The same objective allows the imaging of the trapped GNPs onto CCD

camera (DU897, Andor). SERS spectrums are collected by a commercial spectrometer (Acton SP2300, Princeton Instrument) equipped with a charge-coupled device (CCD) (DU970N, Andor) for analysis. During the experiments, the Raman scattering light passes a notch filter, used to remove the laser line, and is then directed to the desired ports of the microscope for spectral measurements. The first spectrum of the Raman scattering is measured 10 s after the start of the laser irradiation. This 10 s is the waiting time for trapping of enough GNPs and ensures that the particles are saturated at the spot. Without interruption of the laser irradiation, the laser intensity is being changed quickly to the next power, and immediately the second spectrum is measured with the same integration time.

Electrodynamics Simulations: The optical forces are calculated by integrating the Maxwell stress tensor over the surface of the sphere.² The time-averaged Maxwell's stress tensor (MST) is given by $\langle \mathbf{T} \rangle = \frac{1}{2} \text{Re}[\epsilon \mathbf{E} \mathbf{E}^* + \frac{1}{\mu} \mathbf{B} \mathbf{B}^* - \frac{1}{2} \cdot \mathbf{I} \cdot (\epsilon |\mathbf{E}|^2 + \frac{1}{\mu} |\mathbf{B}|^2)]$, which we want to integrate over the surface of the sphere in the following way: $\langle \mathbf{F} \rangle = \iint_S \langle \mathbf{T} \rangle \cdot \mathbf{n} dS$, Where s is any arbitrary surface containing only the particles, \mathbf{n} is the outer unit normal vector to this surface, and dS is a differential element of surface area. In this paper, the electric and magnetic field distributions of the system are numerically calculated using a commercially available FEM package (COMSOL Multiphysics 5.2 with RF module). In all calculations, the permittivity of gold is modeled using the experimental data of Johnson and Christy with linear interpolation,³ and the refractive index of water is taken as 1.33. In order to simulate the infinite air region, the computation domain is truncated by perfectly matched layers to reduce reflections. The simulation domain is finely meshed with a mesh size of 0.1 nm in the gap region such that the convergence of the results and the accuracy of the computed fields are ensured.

SI-2. Aggregation of gold nanoparticles in an optical trap

Movie S1 demonstrates the aggregation of 20 nm gold nanoparticles (GNPs) in an optical trap operating at $\lambda = 1064$ nm. Note more and more nanoparticles are successively approaching to the trap region. However, if the laser beam is blocked, the trapped aggregates fall apart and float away due to Brownian motion.

Movie S2 shows heating and bubbling effect while trapping large (micro) aggregates when using higher power (~500mW).

SI-3. Calculation of interparticle interaction potentials

The classical DLVO theory⁴ states that the DLVO potential (U_{DLVO}) between two GNPs can be expressed as the sum of the electrostatic repulsion (U_C) and the van der Waals attraction (U_{vdW}). For small surface-to-surface separations d we have $U_C \approx 4\pi\epsilon a\varphi_d^2 e^{-d/\lambda_D}$, where $\epsilon = 80\epsilon_0$ is the dielectric constant of water, $a = 10$ nm is the GNP radius and φ_d is the surface potential. The van der Waals attraction potential (U_{vdW}) between the two particles can be expressed as $U_{vdW} \approx -Aa/12d$. Here, A is the materials specific Hamaker constant characterizing the gold-gold interaction mediated through water. The parameter values for calculations were set as follows: effective Hamaker constant, $A = 2.5$ eV;⁵ particle surface potential (zeta potential), $\varphi_d = -53$ mV; and Debye length, $\lambda_D = 5.5$ nm.⁶ The interparticle optical potential (U_{opt}) is calculated using the Maxwell's stress tensor formalism combined with finite-difference time-domain (FDTD) technique,² while treating the intensity I of the incident laser light as an adjustable parameter.

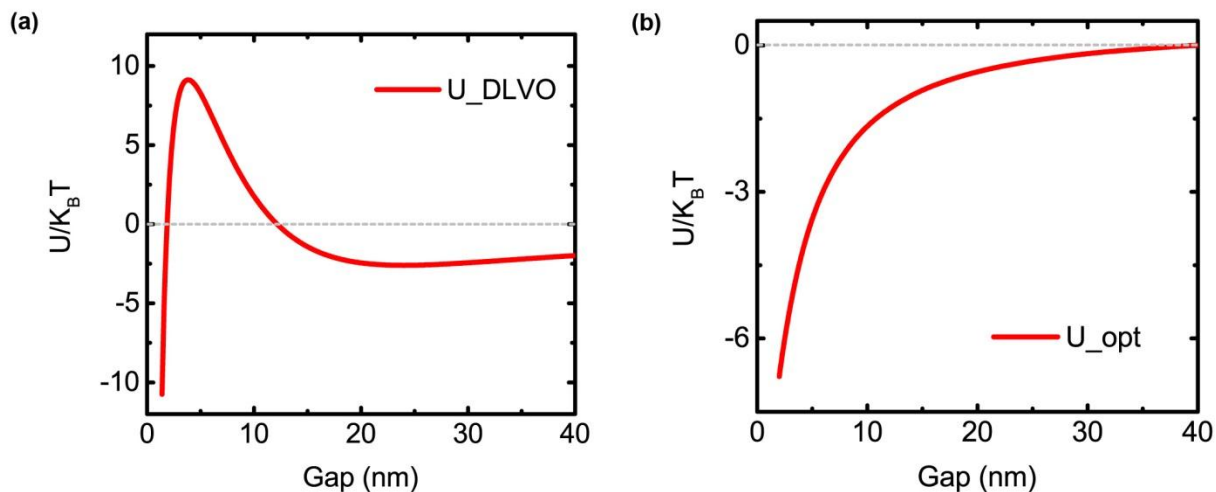


Figure S1. Calculated DLVO (a) and optical potentials (b) versus gap distance in units of $k_B T$ ($T = 300$ K) for a gold dimer system in water illuminated with a plane wave polarized parallel to the symmetry axes.

SI-4. Concentration dependence of Raman scattering intensity for CV

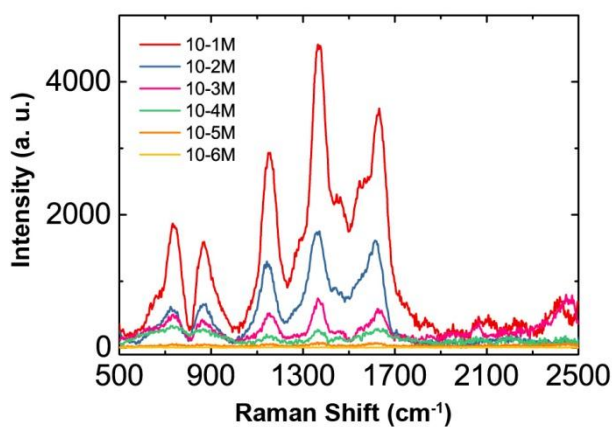


Figure S2. Concentration dependence of Raman scattering intensity for CV in the absence of GNPs at 532 nm excitation. Spectra are obtained with a 10 s integration time. Laser power $\sim 2.5 \times 10^3$ W/cm².

SI-5. Measured Raman spectra with increasing power intensity

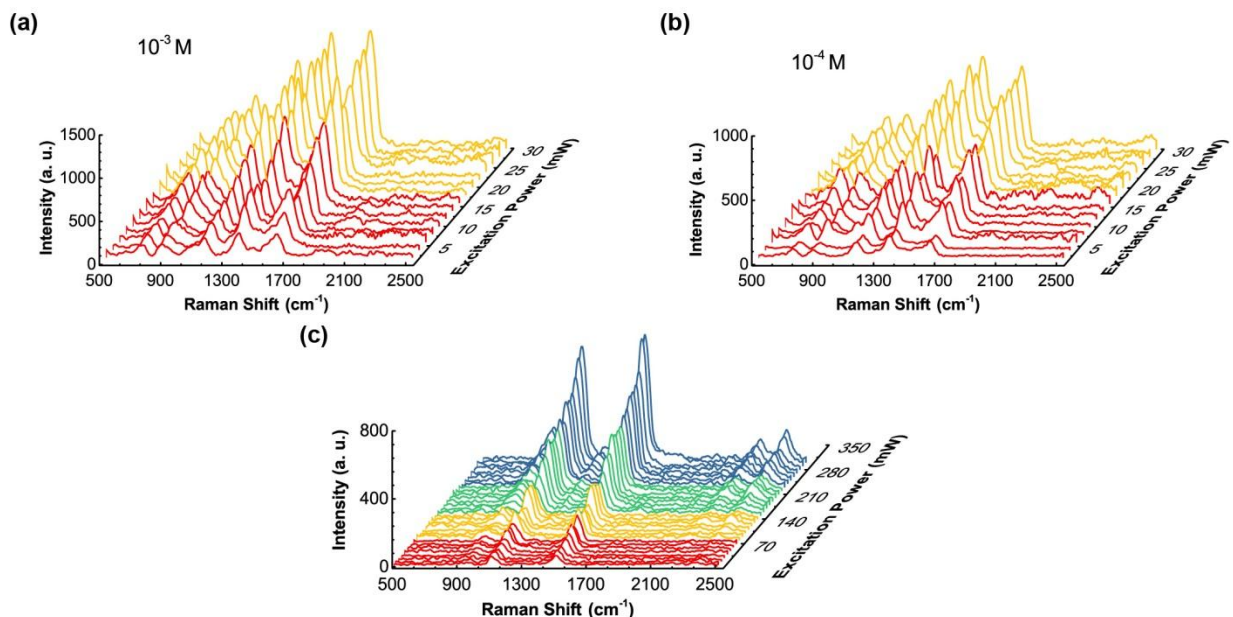


Figure S3. Measured Raman spectra from, 10⁻³ M (a) 10⁻⁴ M (b) and 10⁻⁶ M (c) CV solution including gold nanoparticles with increasing power intensity of 532 nm laser with (c) and without (a, b) the macroscopic trap (1064 nm). Integration time ~ 1 s. The 532 nm laser is polarized in (a, b) and circular polarized in (c).

SI-6. Calculated enhancement factor and far-field scattering for a gold dimer system

We adopt the finite-difference time domain (FDTD) method to calculate the far-field scattering and electric field distribution of the two systems. Fig. S4 indicates that the simple electrostatic model $M \approx (D/d + 1)^2$ gives an excellent quantitative estimate of the interparticle coupling effect. The calculations show that the field enhancement factor is extremely sensitive to the gap distance and the near field is drastically confined and enhanced in the junction as the gap is 2 nm. The features of near field distribution can reflect the SERS enhancement factor, which is roughly estimated as $|E_{loc}/E_0|^4$. The calculations have been performed for different polarizations at

$\lambda = 532$ nm. Note that the enhancement is almost always below unity (i.e. no enhancement) when the polarization of the incident field is perpendicular to the dimer axis.

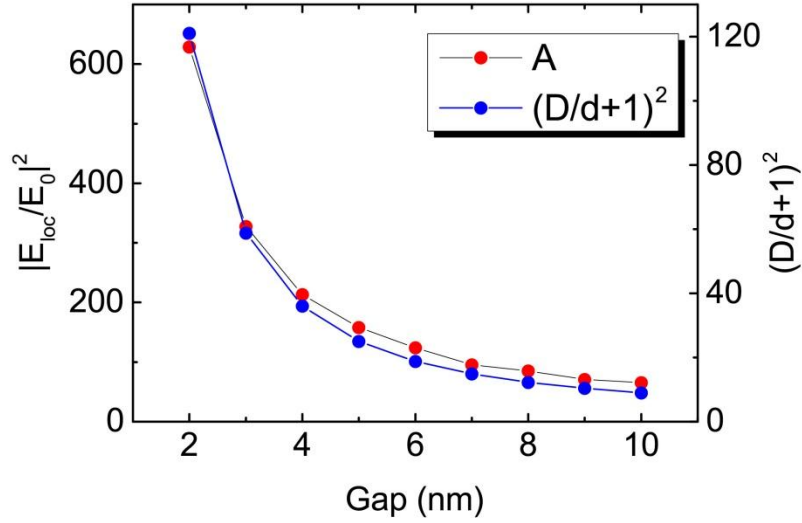


Figure S4. Near field intensity ($|E_{\text{loc}}/E_0|^2$) versus gap distance for a dimer of 20 nm GNPs excited by a 532 nm wavelength plane wave polarized parallel to the dimer axis. Red circle refer to electrodynamic simulations at the position located 0.5 nm from the surface of one of the spheres, while the blue circle is an estimate of the gap enhancement factor based on the “voltage division” model $(D/d+1)^2$.

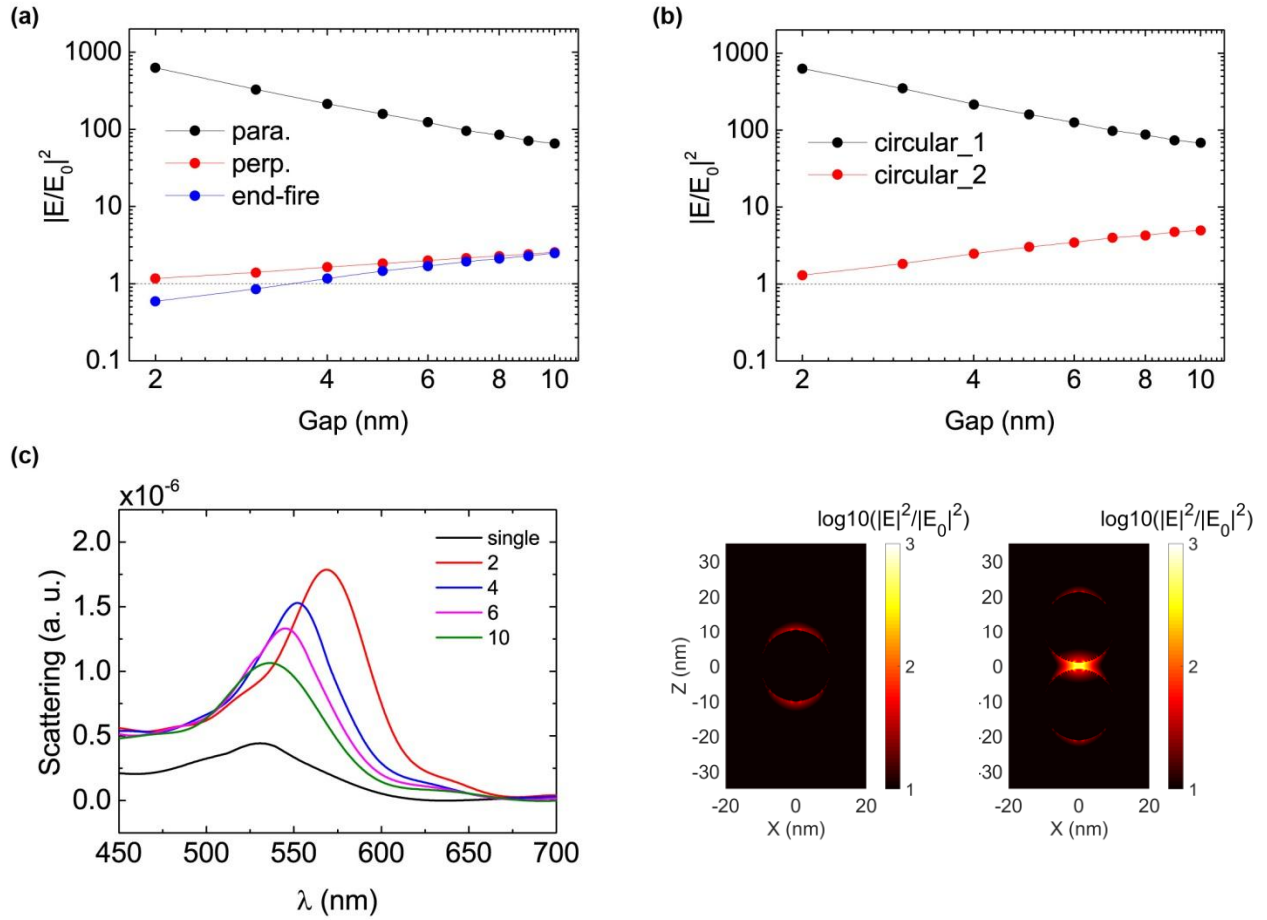


Figure S5. (a) Calculated electric field enhancement factor (EF) for a gold dimer system in the parallel (black), perpendicular (red) and end-fire (blue) polarization configuration as a function of interparticle separation d . (b) Calculated electric field EF for a gold dimer system at 532 nm excitation with circular polarized incident normal to the dimer surface (black) and along the dimer surface (red), respectively. (c) Evolution of simulated scattering spectra of the gold nanospheres in the spectral range of 0.45 ~ 0.7 μm with decreasing gap distance. (d) Electric field intensity distributions for a single GNR and a GNR dimer with gap = 2 nm. The GNR diameter is 20 nm. The calculations in (a, b) have been performed for the position located 0.5 nm from the surface of one of the spheres.

SI-7. The polarization relationship between the Raman spectrum and 1064 nm laser

In Fig. S6 (a, b), we demonstrate the SERS signals from 10^{-6} M CV solution including GNPs as a function of the angle of rotation of the Raman polarization, taken with 532 nm excitation with 90° polarized while with 30° (a) and 90° (b) polarization of 1064 nm laser, respectively. It can be seen that the influence of the polarization state of the 1064 nm laser can hardly influence the results because the total intensity of the scattered light is always maximized along the direction of the 532 nm polarization. This can be understood in the following: the power of the trapping laser (1064 nm) at the sample is ~ 40 mW and the beam waist is adjusted to be of the order 2–3 μm in diameter. The trap volume is thus much larger than the particle size, which ensures that the particle separation is determined by the interparticle interaction rather than by the size and shape of the laser focus. So the polarization state of laser matters only when it can induce attractive interparticle interaction. In Fig. S6 (c), we also provide the numerical calculation far away from the dimer resonance ($\lambda = 1064$ nm) so that the actual contribution of the plasmon can be assessed. As can be seen that the magnitude of the optical force is much smaller out of the plasmon band at $\lambda = 1064$ nm than at the dimer resonance ($\lambda = 532$ nm) and can be safely neglected. As a result, the polarization of 1064 nm laser does not affect the results of the Raman spectrum.

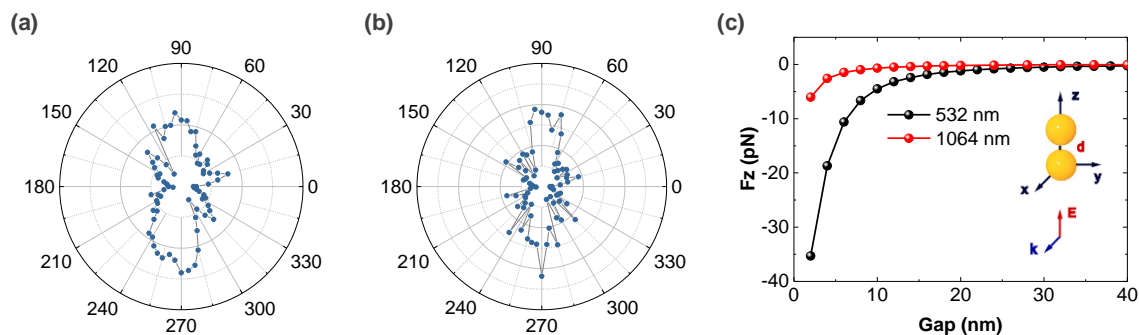


Figure S6. SERS intensity corresponding the peak band (1110 cm^{-1}) from 10^{-6} M CV solution including GNPs as a function of the angle of rotation of the Raman polarization, taken with 532

nm excitation with 90 ° polarized while with 30 °(a) and 90 °(b) polarization of 1064 nm laser, respectively. (c) Calculation of the optical force between two $D = 20$ nm GNPs as a function of the gap distance d at $\lambda = 1064$ nm and at $\lambda = 532$ nm, respectively. The inset depicts schematically illumination configurations for the two-particle (dimer) system in the presence of a plane wave. The wave-vector of the incident wave is denoted by k and its polarization by E . Intensity: $1\text{W}/\mu\text{m}^2$. The polarization of the incident field is parallel to the dimer axis.

SI-8. SERS signals of CV molecule at 10^{-6} M concentration without the macroscopic trap

We experimentally examined the SERS signal of CV molecule at 10^{-6} M concentration without the macroscopic trap (1064 nm). As shown below, the SERS intensity counts significantly reduced to be below 100, which is very weak and almost undetectable, especially for laser power under 50 mW.

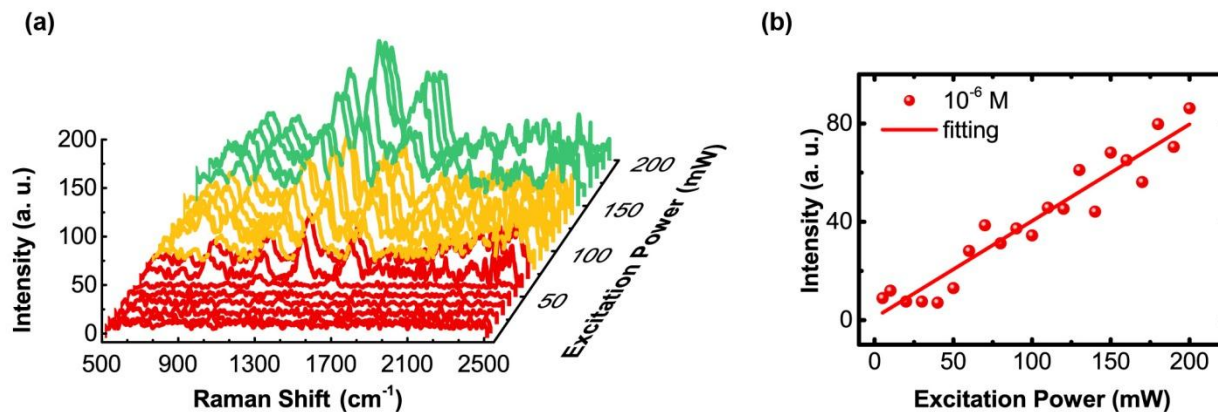


Figure S7. (a) Measured Raman spectra from 10^{-6} M CV solution including GNPs with increasing power intensity of 532 nm laser without the macroscopic trap (1064 nm). Integration time ~ 1 s. (b) Peak heights of the 1147 cm^{-1} line for the Raman spectra as a function of excitation power at $\lambda = 532$ nm. The solid line is the linear fit.

SI-9. Time-fluctuating of SERS signals For a 10^{-7} M concentration CV solution.

Figure S8 presents the time dependence of the total intensity of Raman scattering for CV molecules of 10^{-7} M concentration illuminated at $\lambda = 532$ nm with different laser intensity. Each row represents one laser power, whose scattering intensity was obtained by integration of the Raman spectra.

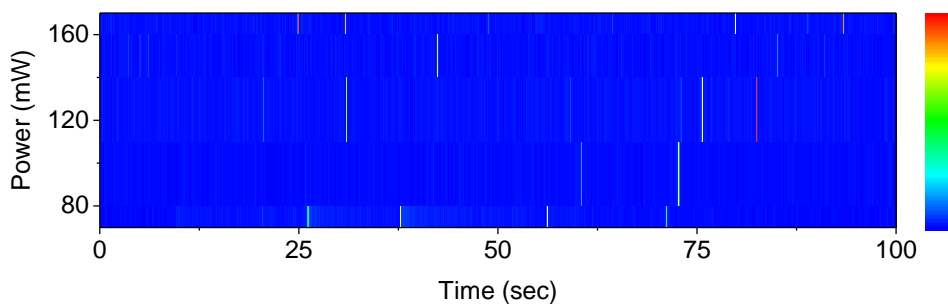


Figure. S8. Intensity trajectories for CV molecules of 10^{-7} M concentration illuminated at $\lambda = 532$ nm with excitation power of 70, 90, 130, 150 and 170 mW, respectively. The intensity corresponds to peak heights of the 1110 cm^{-1} line for the SERS spectra.

SI-10. Experimental setup

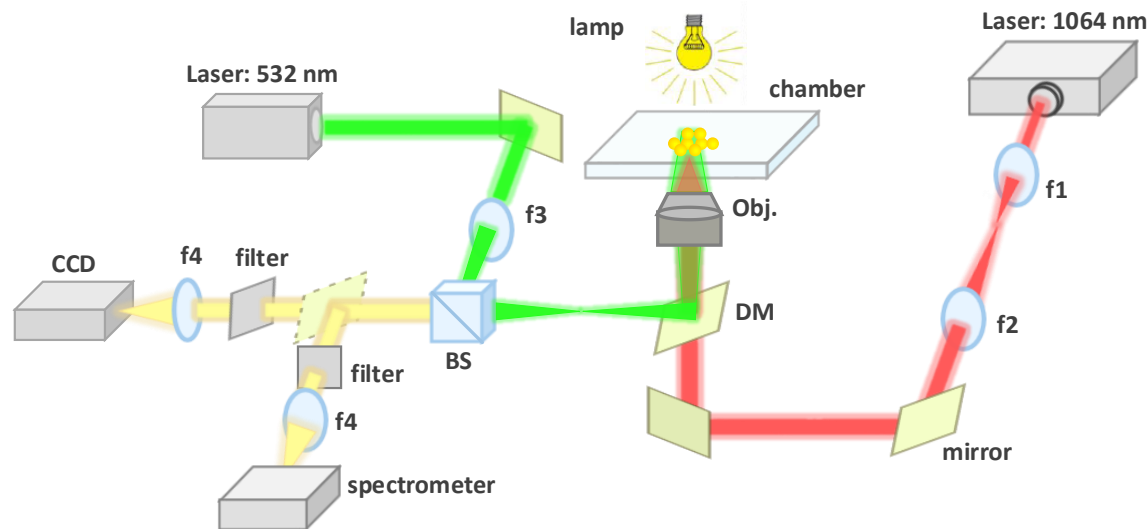


Figure S9. Schematic of the experimental setup. The beam telescope send the laser to slightly overfill the back aperture of the high-NA (1.25) trapping objective, which focuses the beam into the chamber. Lens f3 ($f = 60$ mm) is used to separate the focal plane of 532 nm laser and 1064 nm laser. The trapping and aggregation are observed with a charge coupled device (CCD) camera and SERS spectrums are collected by a commercial spectrometer. Another lens (f4) is placed in front of the camera in order to observe the image at the focus of the objective lens. The lamp on the right top is used for imaging. The green light (532 nm) is filtered out by a notch filter.

REFERENCES

1. L. Brey, G. Schuster and H. Drickamer, *J. Chem. Phys.*, 1977, **67**, 5763-5765.
2. L. Novotny, in *Near-field optics and surface plasmon polaritons*, Springer, 2001, pp. 123-141.
3. P. B. Johnson and R.-W. Christy, *Phys. Rev. B*, 1972, **6**, 4370.
4. D. J. Shaw, *Introduction to colloid and surface chemistry* 1980.
5. J. N. Israelachvili, *Intermolecular and surface forces* 1985.
6. Y. Tanaka, H. Yoshikawa, T. Itoh and M. Ishikawa, *Opt. Express*, 2009, **17**, 18760-18767.